Transient Gulf Stream Meandering. Part I: An Observational Experiment[1]

A. R. ROBINSON

Center for Earth and Planetary Physics, Harvard University, Cambridge, Mass. 02138

J. R. LUYTEN AND F. C. FUGLISTER

Woods Hole Oceanographic Institution, Woods Hole, Mass. 02543

(Manuscript received 18 June 1973, in revised form 17 October 1973)

ABSTRACT

The results from an observational experiment on the mesoscale space-time variability of the Gulf Stream are reported. Various techniques, including aerial surveys, ship trackings of the 15C isotherm at 200 m, drogues and moored current meters were used and are compared, to give estimates of the variability of the motion over a wide range of scales. A two-week time series of daily tracks of the Stream near 70W are used to interpolate instantaneous paths over 2° of longitude. These paths provide the first detailed information on the small-scale variability of the path indicator of the Gulf Stream northeast of Cape Hatteras. Similarly, the long time series of triweekly aerial surveys provides a detailed picture of the evolution of a large-scale meander.

1. Introduction

Observations of the Gulf Stream over many years have shown that the narrow intense current and its associated horizontal density contrast moves about coherently in the open ocean as a recognizable structure. The precise manner in which it changes its position and the range of scales of space and time variability have been a subject of much interest. As with many geophysical phenomena, the Gulf Stream exhibits variability over decades of scales, ranging from its primary decay scale, essentially its length, of many thousands of kilometers, through the intermediate scales associated with the local behavior of the path and ring vortex-shedding, to scales on the order of the width, some tens of kilometers (see Table 1). The observations reported here were designed to explore and define the intermediate-scale variability in both space and time, usually referred to as meandering. Sampling rates required for the above purposes necessarily yielded the first information on smaller scales.

In the summer of 1969, a joint observational experiment was undertaken by Harvard University, the Woods Hole Oceanographic Institution and NAVOCEANO to examine the mesoscale space-time variability of the Gulf Stream by various techniques. Toward the end of May, and continuing until 1 August, a series of aerial surveys of the maximum surface temperature gradient was made between Cape Hatteras and 65W, which delineated the large-scale variability of the surface outcroppings or the extreme shoreward extension of the Stream. In June four bottom moorings with current meters at 200 m from the ocean floor were set along 70W between 36°23′N and 37°20′N. The current meters were recovered in August with a 65% data recovery. The R/V *Chain* was in the vicinity of the Stream between 26 June and 21 July. A hydrographic section of the stream was occupied along 70W to determine the transport and momentum flux of the Stream. A two-week series of tracks, over 2° of longitude, of the 15C isotherm at 200 m depth, a marker for the maximum horizontal density gradient of the Stream, was made to determine the variability of the position, direction and curvature of the Stream path. Near-surface drogues were tracked together with a simultaneous determination of the near-surface (200 m) temperature gradient to examine the correspondence between the maximum current and the thermal structure. A composite of these data is shown in Fig. 1. In this paper we report these data and discuss their interrelations and intercomparisons.

The philosophy underlying the planning of this experiment has been discussed by Robinson (1971); an

TABLE 1. Gulf stream space and time variability.

Regime	Length scale (km)	Time scale (days)	Velocity scale (cm sec^{-1})
Secular change	250	13±3	0–8
Large-scale variations	40	~1	22±4
Small-scale variations	20–30	3±1	5±2

[1] Contribution No. 3120 of the Woods Hole Oceanographic Institution.

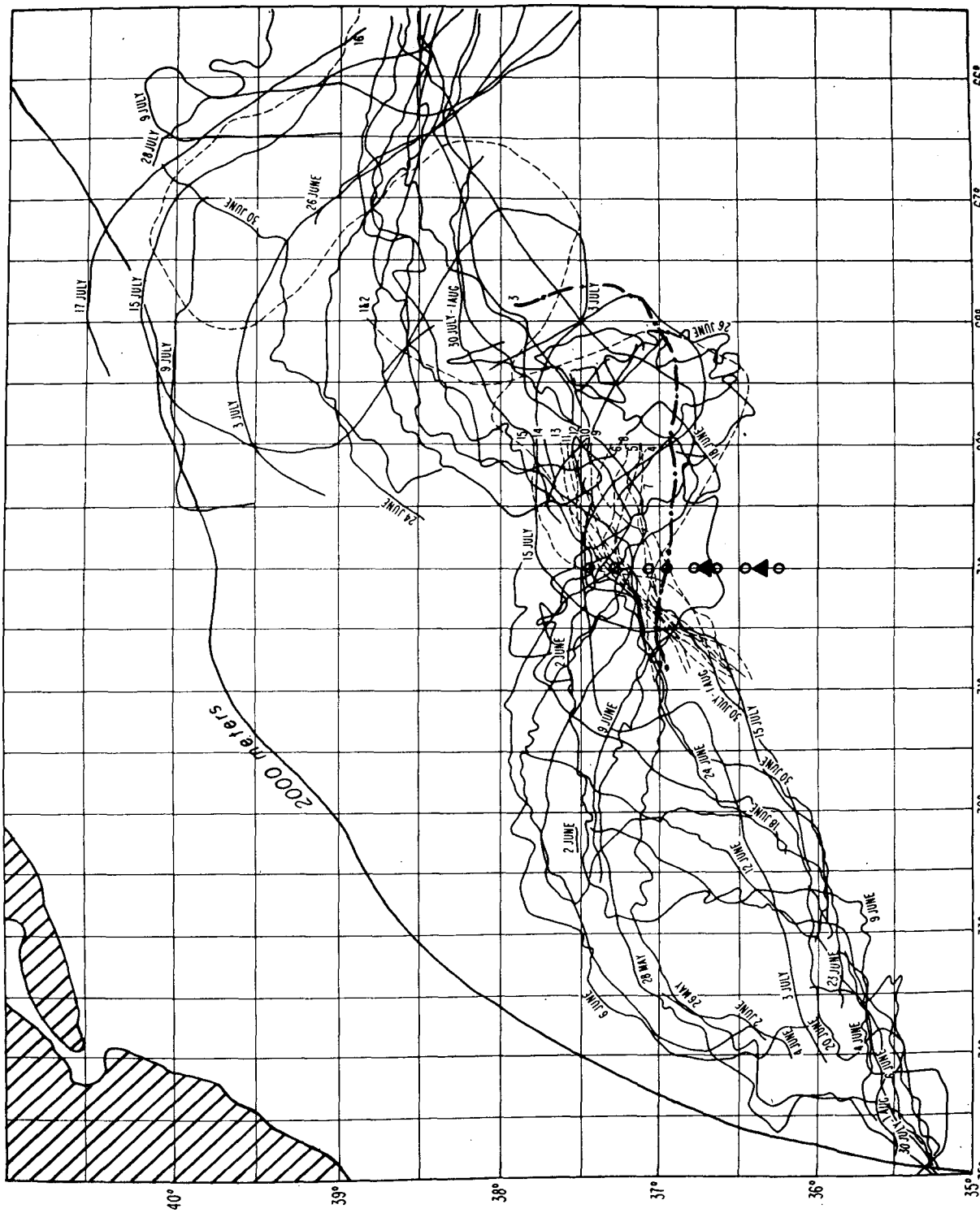

FIG. 1. Composite of path data (shiptracks, dashed lines; airtracks, solid lines; drogues, dash-dotted lines) and location of current meters (×) and hydrographic stations (○).

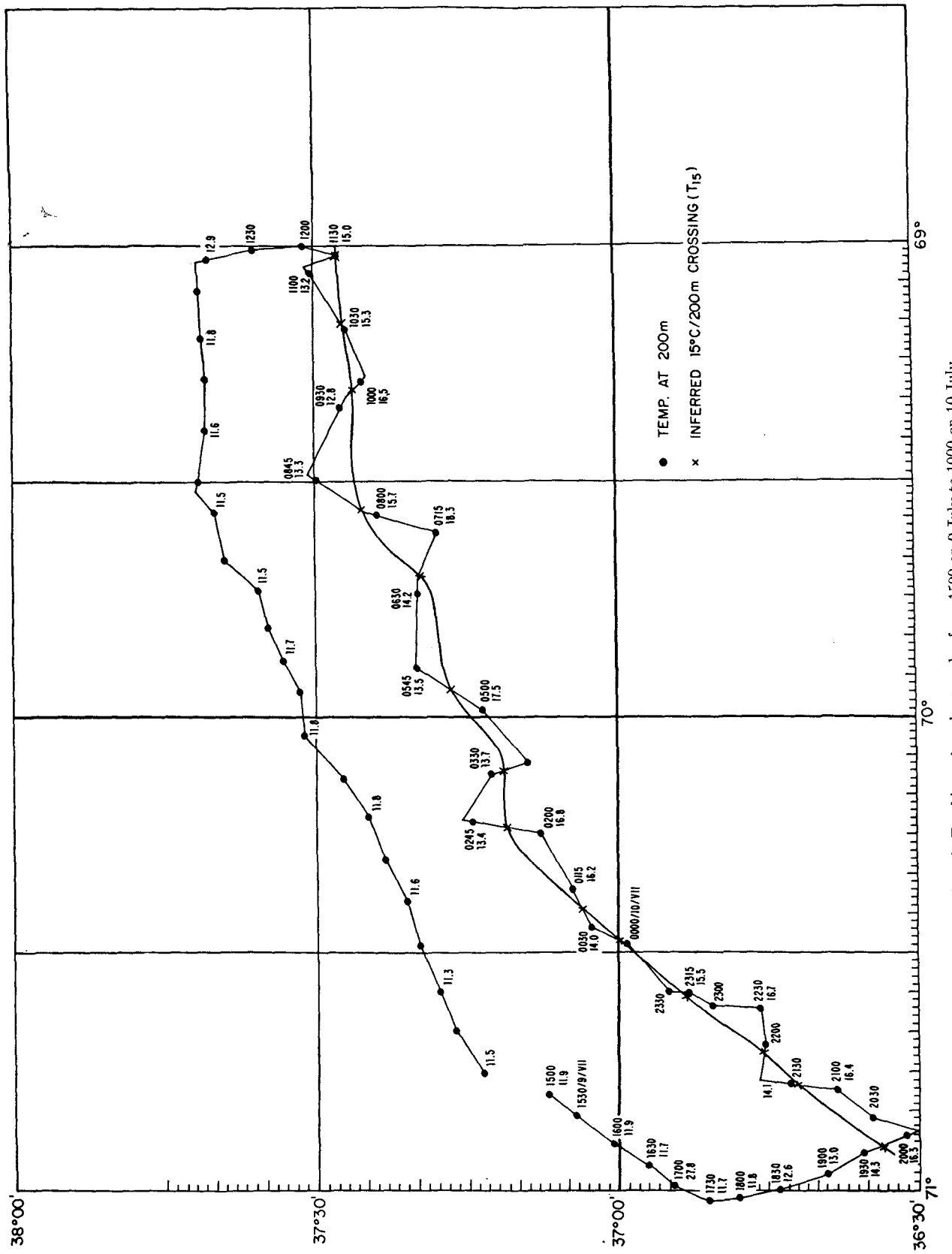

FIG. 2. T_{15}-shiptrack and return leg from 1500 on 9 July to 1000 on 10 July.

attempt was made to gather a variety of data, sufficient to determine the local dynamics of the meandering process. The necessary initial and inlet conditions, together with the basic parameters of a theoretical model of the Stream, were gathered to be able to calculate the evolution of the path, which could then be compared with the observed evolution of the path. We shall report in a subsequent paper [Part II of this study (Luyten and Robinson, 1974)] the interpretation of these data via a theoretical model of the meanderings which, in turn, grew out of these observations (Robinson *et al.*, 1973).

These observations are discussed below, first from a qualitative point of view and second from a quantitative point of view. The primary data on the path of the Stream, and the direct velocity measurements are discussed in Section 2. An analysis of the sources of error in these data which relate to estimates of the scales of motion is given in Section 3. The intercomparisons between the complementary techniques, together with the quantitative estimates of the scales of space-time variability of the Stream, are discussed in Section 4.

2. The observations

In this section we shall discuss the primary data from all of the various parts of the observational program, together with the overall qualitative interpretation. Detailed discussion of these data will be deferred to subsequent sections.

a. Shiptracks

The thermal structure in the near-surface layer along a section perpendicular to the Stream always shows a close packing of isotherms indicative of the strong horizontal density gradient associated with the Gulf Stream current. Various detailed studies have shown the correspondence between the strong velocity core of the Stream and the sharp horizontal density gradient as marked by the position of the 15C isotherm at 200 m depth (Fuglister and Voorhis, 1965; Hansen, 1970). This near-surface Stream indicator will be referred to as T_{15} and is used to identify the position of the axis of the Gulf Stream.

The path of the Stream was determined by altering the ship's course between successive half-hourly XBT

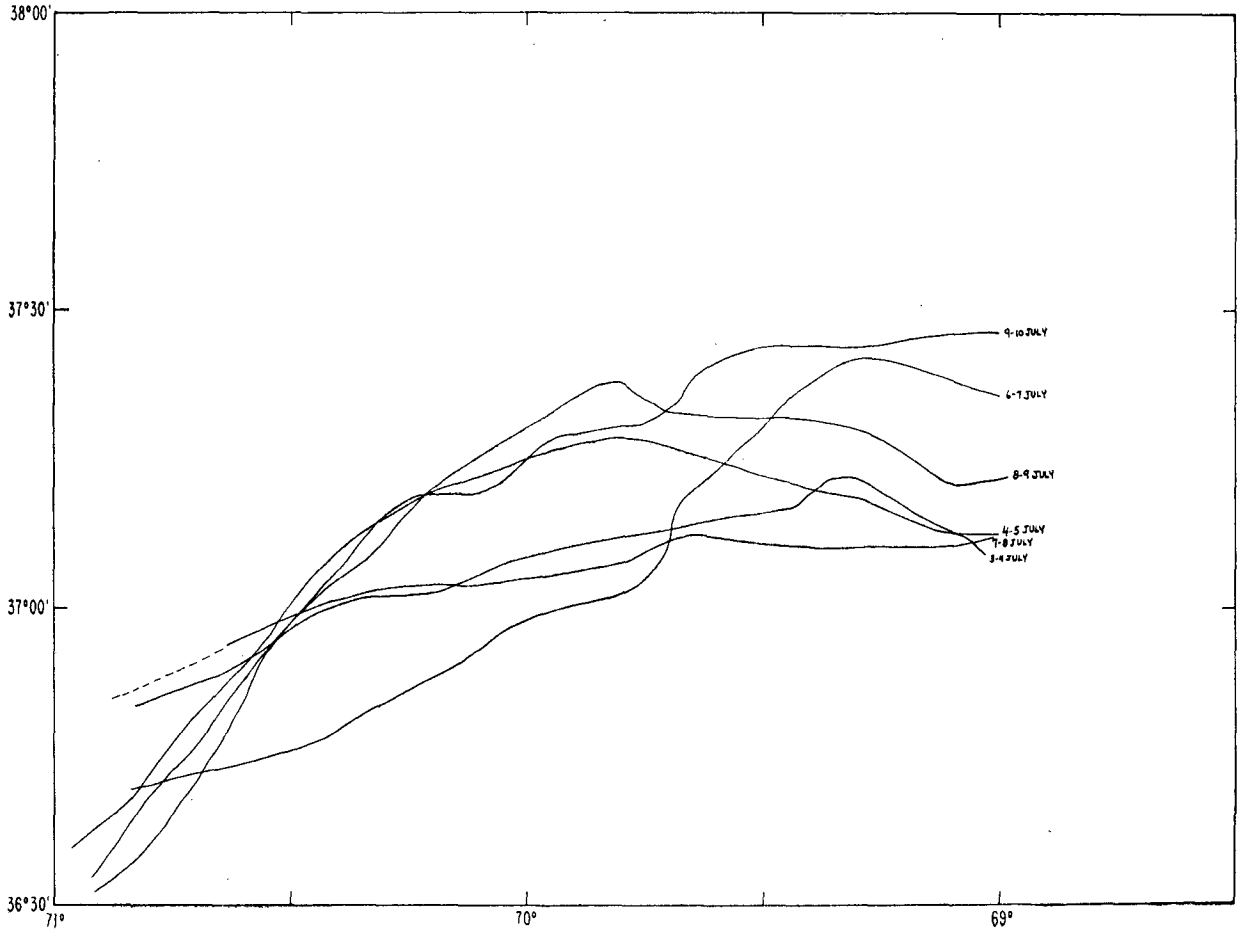

FIG. 3a. Composite of shiptracks over the period 3–10 July.

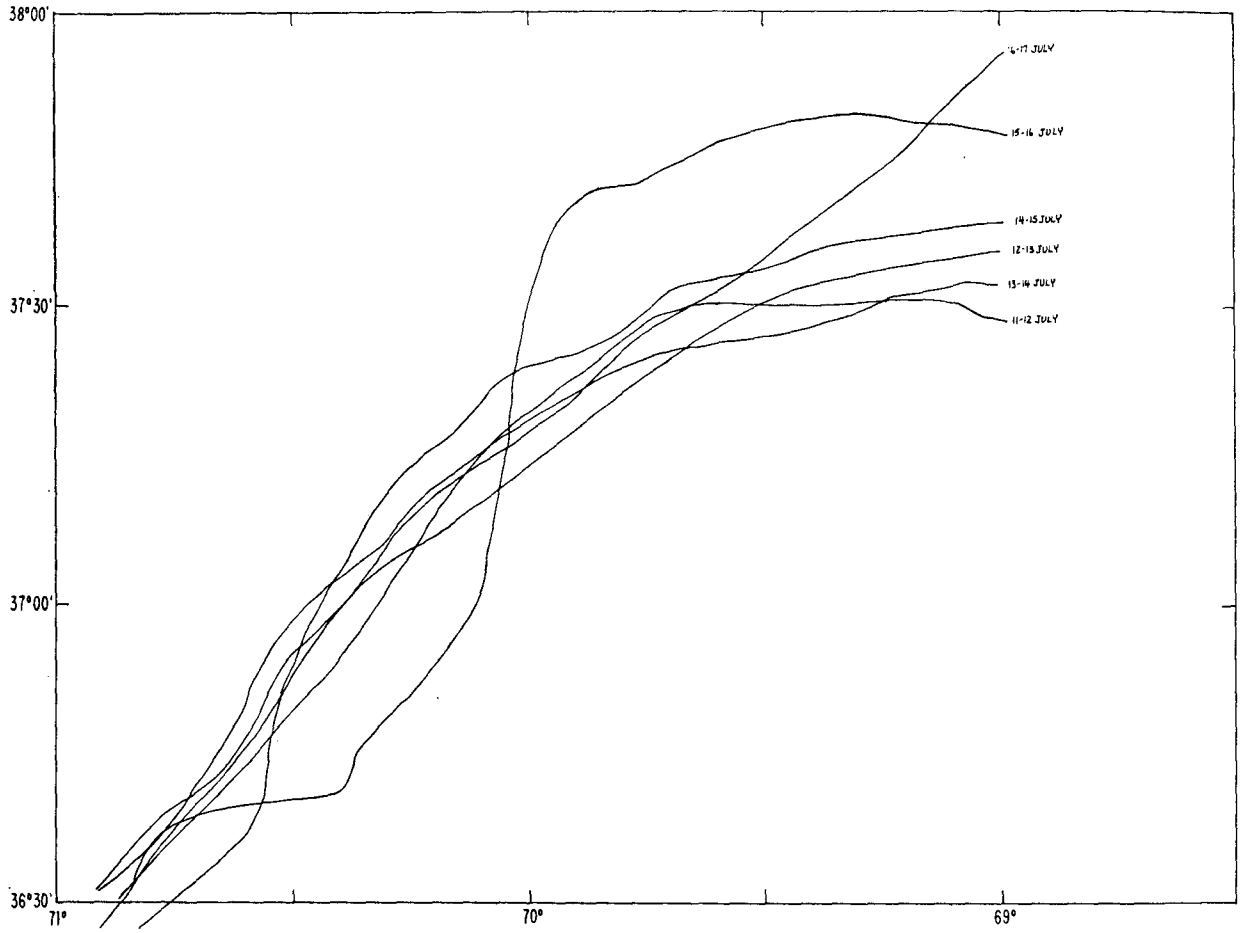

FIG. 3b. As in 3a except for the period 11–17 July.

stations, bracketing T_{15} as often as possible. A linear interpolation along the ship's track was made to determine T_{15} and obtain a track of the path of the Stream. To avoid cumbersome usage, we shall use the expression *shiptrack* to refer to the line interpolated through the set of T_{15} positions determined along the ship's path. This definition is required because we will subsequently by space-time interpolation construct instantaneous paths of the Stream. The shiptrack, together with the 200 m temperatures and the ship's path for 9 July, shown in Fig. 2, indicates the ability of this technique to resolve the small-scale features in the path, discussed in Section 4a. Although there may always be some aliasing, this technique appears to resolve the dominant and persistent variability adequately.

The R/V *Chain* made fourteen tracks of T_{15} in the vicinity of 70W. Two long tracks were made from 71W to 68W, at the beginning of the cruise (25 June–3 July), and a third long track from 71W out to 64W at the end of the cruise (17–20 July). Eleven shiptracks were made successively in the region between 71W and 69W in the period 4–17 July.

The short tracks required 11 hr, on the average, to make and the return leg to 71W took 15–16 hr. Thus, the position of the Stream was determined repeatedly between 71W and 69W every 26 hr. A composite of these short tracks displayed in Fig. 3 illustrates the variability of the position and heading over a range of scales.

The three long paths, shown in Fig. 4, illustrate a cyclonic movement of a rather sharp bend of the Stream axis. This movement, together with the overall change in heading of the Stream at 70W, are possibly associated with the development of the convoluted shape of the path seen in the third and longest shiptrack of 17–20 July.

b. Airtracks

We present here qualitative features of the series of aerial surveys of the Gulf Stream made between May and August 1969 by NAVOCEANO in cooperation with the Naval Research Laboratory. The qualitative features of these surveys have been discussed by Wilkerson and Noble (1970). We include a discussion of the

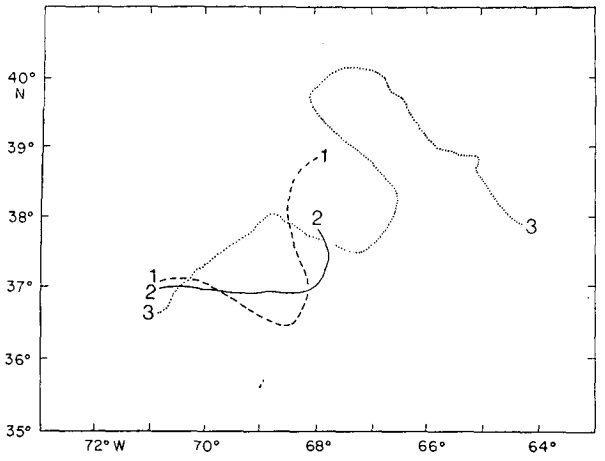

FIG. 4. Composite of three long shiptracks: 1, 25–27 July; 2, 29 June–3 July; 3, 17–20 July.

same nature for completeness and because the data are analyzed quantitatively below. The sharp horizontal gradient of the sea surface temperature (front) delineates the subsurface Gulf Stream axis, characteristically lying about 35 km shoreward or northward (Hansen and Maul, 1970). The position of this gradient, denoted T_s, was determined by airborne radiation thermometry; the line interpolated through a set of these positions is referred to as an airtrack.

The airtracks were started between 75W and 73W, near Cape Hatteras, and the maximum surface temperature gradient was tracked downstream to longitudes between 65W and 60W. The tracks were made about every two days from 26 May until the thermal contrast across the Stream became too weak due to the surface heating of the slope water (1 August). The surface heating results in a change of the particular isotherm associated with ΔT_s from 20C in May to 26C in late July. Secondary thermal fronts of relatively small spatial scale complicate the identification of the Stream.

The airtracks are primarily useful for the observation of the large-scale motions of the path. The development and evolution of a large meander to the east of 70W during the month of June can be observed in Fig. 5. A relative node in the meander pattern was observed near 70W, which was maintained throughout most of the period of observation. The airtracks during July (Fig. 6) show the continued development of the meander until the seasonal heating effects begin to obscure the interpretation.

A plot of the airtracks relative to a rhumb line (Fig. 7) emphasizes the propagation of features in

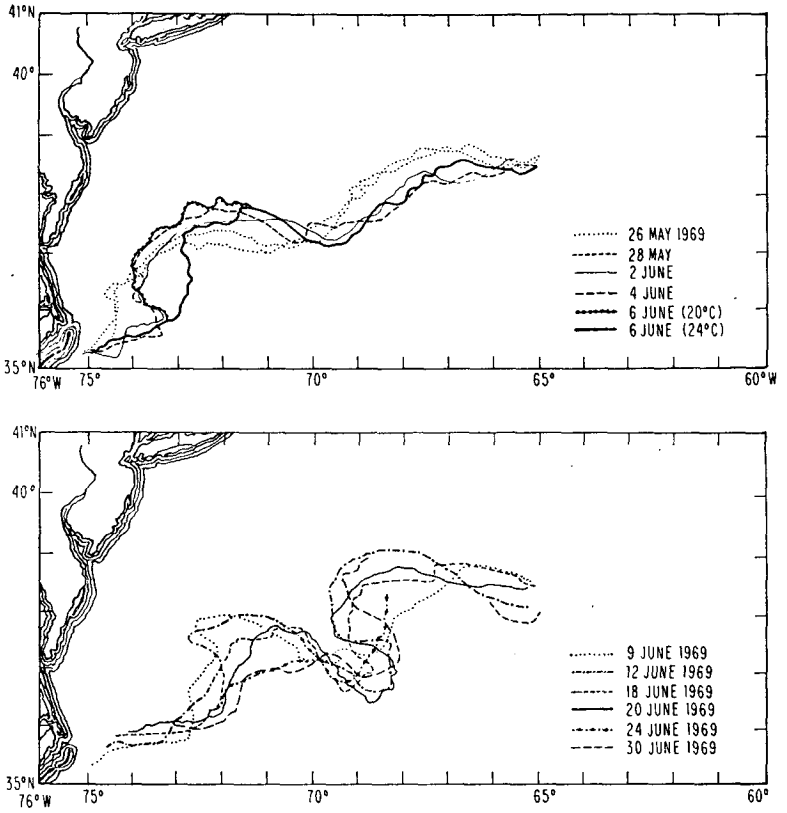

FIG. 5. Composite of airtracks from 26 May–6 June (upper) and 9–30 June (lower).

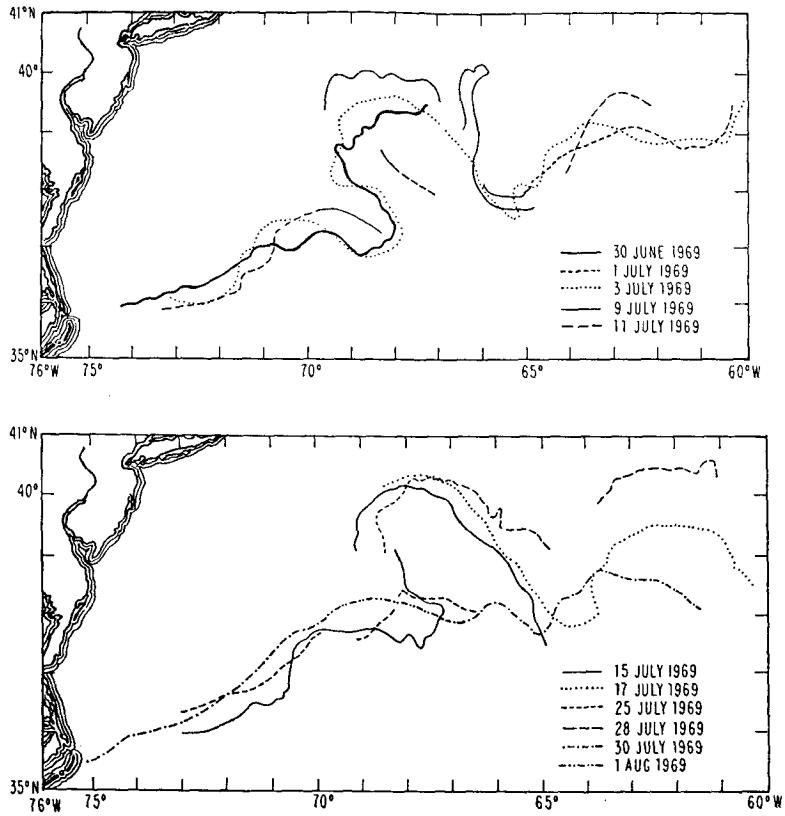

FIG. 6. Composite of airtracks from 30 June–11 July (upper) and 15 July–1 August (lower).

the path structure, rather than the local temporal development of the meander pattern. The basic qualitative picture is the same, showing the nearly stationary development of the large meander, together with a slow eastward propagation of the structure. It is clear from these paths that a sampling rate of two days is needed to detect and resolve the evolution of the meandering Stream even over large scales.

c. *Moored current meters*

An array of four bottom moored current meters was set by W.H.O.I. on 12 June 1969 in a north–south line along 70W with a 35 km spacing from 37°20′N to 36°23′N. The current meters were 200 m from the sea bottom. The two southernmost current meters yielded good records for the two-month period. The position of the array was chosen along 70W because a number of airtracks of the Stream position showed a node in the meander pattern, as indicated in Fig. 8. Over the course of the observations, the node moved 40 km toward the west. The current meter observations and a preliminary comparison with the Gulf Stream position data obtained during this period has been reported by Schmitz *et al.* (1970). We refer the reader to that paper for a discussion of the longer period fluctuations and correlations with other current meter observations. We shall concentrate rather on the shorter time scales limited by the ship observations.

The two current meters with two-month records, denoted 3041 (36°23′N) and 3051 (36°43′N), exhibit similar velocities over the entire record length. The aircraft and ship observations of the position of the Gulf Stream indicate that the Stream axis remained within 70 km of the current meters throughout the observations. Filtered time series of the east and north components from 3041 and 3051, shown in Fig. 9, has been made available to us by W. J. Schmitz (1972, personal communication). The corresponding vectors, plotted once a day, are shown in Fig. 10. Nearly all (95%) of the energy of the inertial and higher frequencies has been removed from the original time series by a Gaussian filter in the time domain.

The current meter records show a great deal of visual coherence of variability although there is little point in computing a statistical coherence estimate between time series whose length is not long compared with the dominant variability. The east component is dominated by variability with a time scale around 10 days whereas the north component contains significant variability at longer scales as well. The vector plot (Fig. 10) emphasizes the longer period fluctuations and clearly

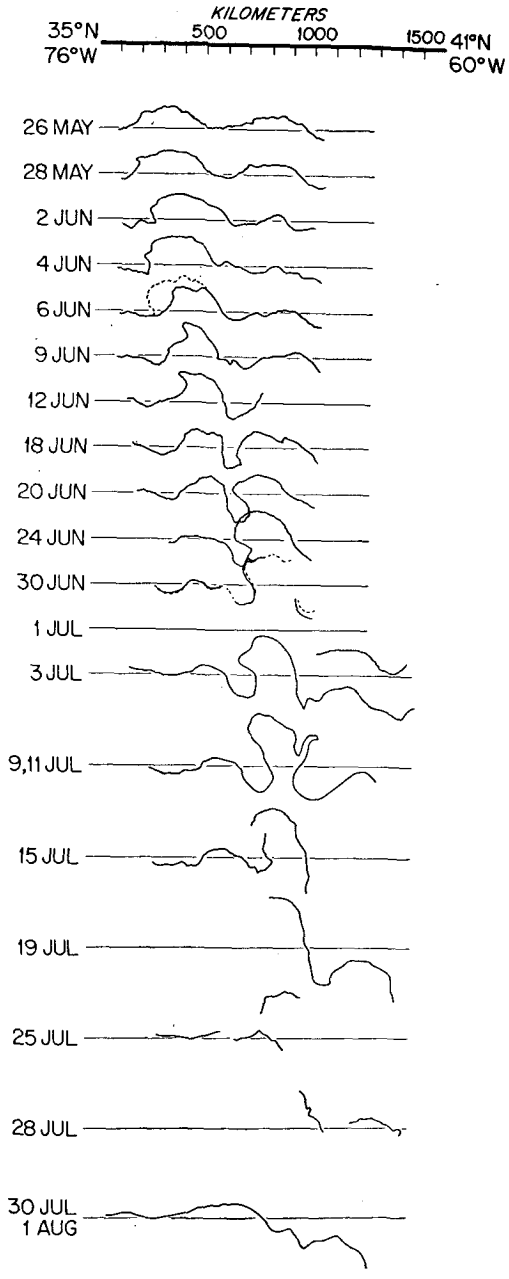

FIG. 7. Airtracks relative to the rhumb line 35N, 76W–41N, 60W. For 6 June both ΔT_s are shown: 24C (solid line), 20C (dashed line). T_s is associated with 20C prior to 6 June, and with 24C after that.

demonstrates the visual coherence, as vector fields, between these records. The maximum observed speed was 44 cm sec^{-1}, the minimum 4 cm sec^{-1}, and a mean speed of 23 cm sec^{-1}. Bottom velocities of this magnitude have not previously been reported, with the exception of a Swallow float observed on the *Aries* expedition (Swallow, 1971; Crease, 1962). A two-day average velocity of 41 cm sec^{-1} was reported at a depth of 4 km. These observations were made in a region where the Gulf Stream may have penetrated although no determination of the Stream's position was made (Hansen, 1970). A more detailed comparison between the bottom currents and the motion of the Stream is made in Section 4a.

d. Drogue measurements

Two near-surface drogues were tracked in the Stream for a total of 63 hr over a downstream range of 430 km. The position of the drogue was determined from a radar range and bearing on the float together with a Loran fix on the ship. A simultaneous track of T_{15} was made. A description of the drogue, together with observations in the Gulf Stream made at other times, has been given by Parker (1972).

The drogues were launched as close as possible (1 km) to the position of T_{15}. The first drogue was recovered 5 hr after launch because the radio had failed; a second was launched immediately. The second drogue was tracked for 58 hr over $2\frac{1}{2}°$ of longitude along the Stream.

The simultaneous track of T_{15} is coincident with the path of the drogue to within observational errors (Fig. 11). The mean separation between T_{15} and the drogue, 1.5 km, was exceeded on about 10% of the fixes along the track.

The motion of the drogue system as a whole is determined by the condition that there is no net force normal to the line at any point. When this condition is integrated over the length of the line, the velocity of the drogue is determined in terms of an average of the velocity in the upper 200 m of the sea. The observed mean speed of 190 cm sec$^{-1}\pm$25 cm sec^{-1} agrees well with the typical values of 200 cm sec^{-1} obtained from ship drift and GEK observations (Worthington, 1954).

This coincidence with the thermal indicator of the Stream, T_{15}, indicates that there is no relative motion between the drogue and the "thermal path" of the Stream. This supports the idea that the thermal and velocity structures of the Stream essentially coincide. This is additional evidence for the use of the thermal structure to mark the velocity structure of the Stream, the axis of the Stream being that line where there is no relative motion normal to the axis.

e. Hydrographic section

A standard hydrographic section across the Gulf Stream was occupied by the *Chain* along 70W between 28 June (1400) and 30 June (0120). Eight deep stations were taken, bracketing each of the four bottom moored current meters. The station separation was approximately 20 km with a total separation of 130 km. Five of the eight deep casts were within 200 m of the bottom, with the remaining three having much larger wire angles so that the bottom bottle was at some 400 m from the bottom.

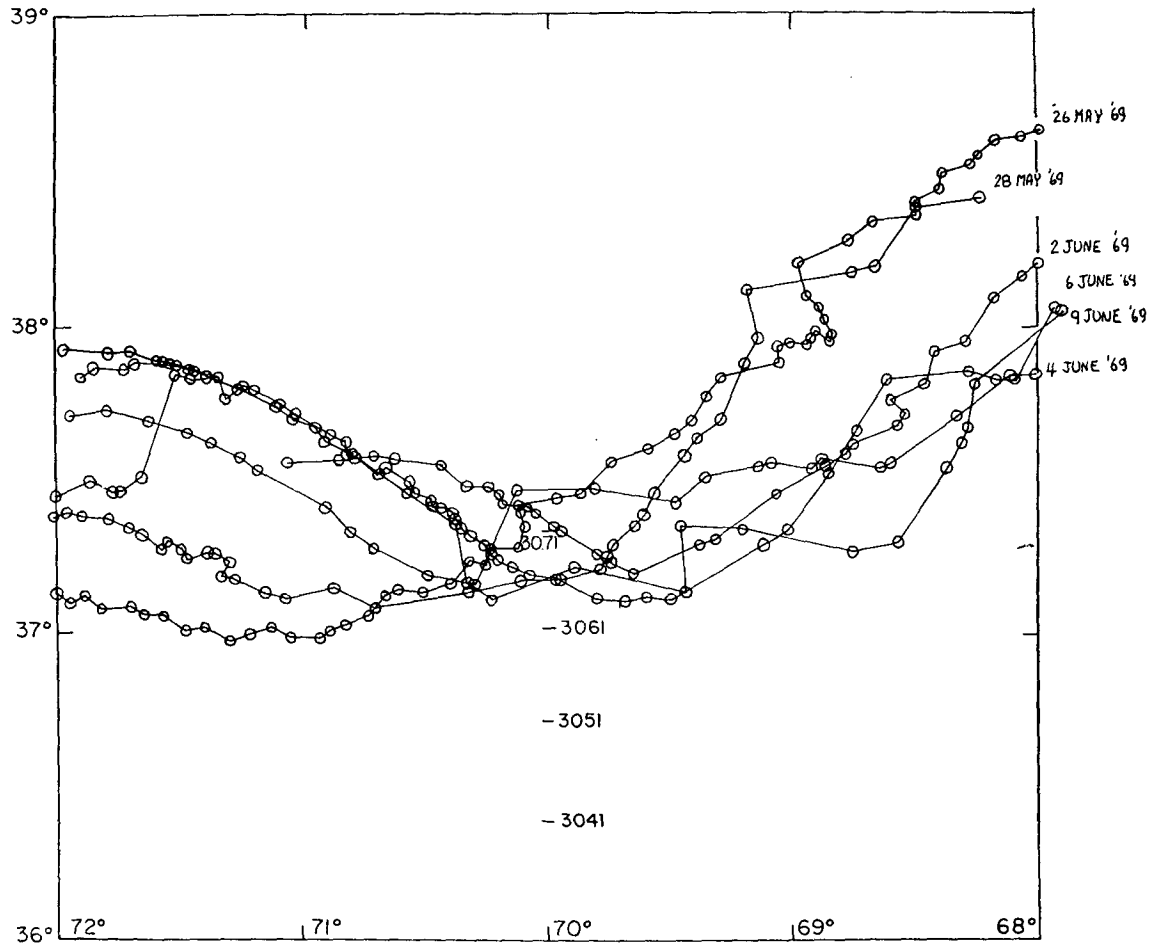

FIG. 8. Node in airtracks between 26 May–9 June in relation to the current meter positions.

Several shiptracks of T_{15} were made a few days before and after the section was occupied. Two isolated fixes on the Stream axis were obtained just before and during the section. Unfortunately, these data, shown in Fig. 12, are not sufficient to give an unambiguous picture of the motion of the Stream during the section, but they will be used to set limits of error.

In this section we have presented the raw data with which the rest of the paper is concerned. There are many intercomparisons to be made among the various types of data. These will be examined in the following sections.

3. Error analysis

There are a variety of sources of error in the data. We shall discuss them and their magnitudes in this section and we shall present estimates of the error implicit in various quantities derived from the primary data.

Common to all of the observations are the navigational errors associated with the determination of the ship's position. In the region between 71 and 69W, 36 and 39N, three ground-wave Loran A channels could be used most of the time. Although pairs of Loran signals can drift up to 5 μsec over periods of a month or more, the relative synchronism over periods of days is good. The timing errors typical of ground wave reception are ±2 μsec, corresponding approximately to an error in position of ±2 km in the region of measurement (Pierce, 1971, personal communication). One should perhaps consider the errors with respect to the Loran lines as axes, giving ellipses of error rather than circles of error. Since there are many other sources of error in any of the measurements, this additional precision is unnecessary.

In the shiptracks additional errors are introduced because of the necessity to interpolate the position T_{15} from 200 m temperatures within 3C of 15C, separated by some 15 km. The composite uncertainty in the T_{15} position arising from the linear interpolation, navigational errors, errors in the XBT temperatures and depths, and possible time delays between the temperature sounding and Loran fix is ±3 km, assuming these errors to be random and uncorrelated.

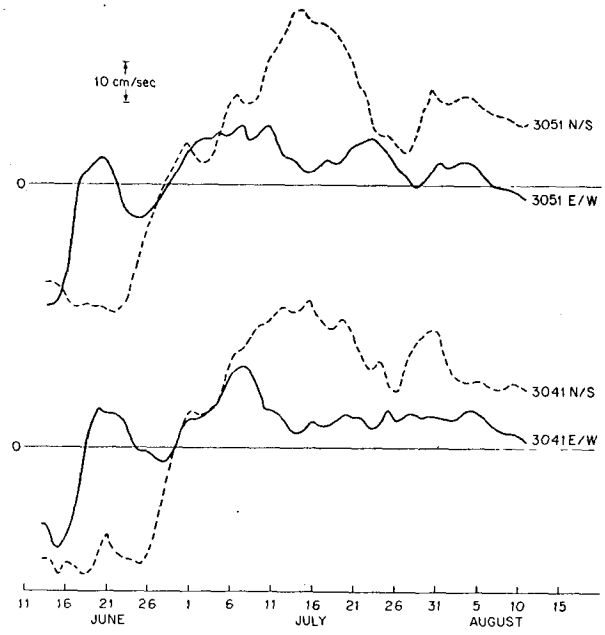

FIG. 9. Low-pass filtered current meter components (north–south and east–west) from moorings 304, 305. Positive values represent northerly and easterly components.

The corresponding errors in the positions of ΔT_s have been estimated by Wilkerson and Noble (1970) to be ± 4 km.

The sources of error in the primary hydrographic data are well known (Warren and Volkmann, 1968) and give rise to uncertainties in computed geostrophic shears of $\pm 10\%$. The maximum errors arising in the geostrophic approximation from the motion of the Stream axis, curvature, and misorientation of the section in this case are estimated to be $\pm 6\%$ (Fomin, 1964). The additional imprecision in transport arising from the ambiguous free seaward edge of the Stream will be discussed in connection with the value of the transport reported.

4. Interpretation and intercomparison

The primary data presented above will be discussed in this section in order to obtain quantitative estimates of the scales of the space-time variability and to delineate the regimes of variability. We shall also define and estimate some non-dimensional parameters that relate to specific dynamical models. In Part II of this study, we shall analyze the relevant data presented here in terms of a quasi-geostrophic model for transient meandering (Luyten and Robinson, 1974).

a. Instantaneous paths

A direct determination of the space and time scales of the motion of the axis of the Gulf Stream is only possible if the measurements can resolve those scales. The interpretation of shiptracks of T_{15} is complicated by the mixing of time and space scales—they are not an instantaneous snap-shot of the path of the Stream since the paths require a finite time to determine. The series of short shiptracks between 71 and 69W is sufficiently dense in time and space to construct a series of paths (T_{15}) at a given time. A plot of the latitude of T_{15} against time for various fixed longitudes is interpolated to give the latitude-longitude relation at given times. This curve is then smoothed to give instantaneous paths of T_{15}. The extent to which the original series of shiptracks resolves the time scales of the motion is measured by the close correspondence between the two sets of paths indicated in Fig. 13. Had we sampled less frequently, many of the smaller scale features would have been lost. For the three long shiptracks, there is no possibility of interpolating instantaneous paths.

The instantaneous paths obtained from the shiptracks between 4 and 17 July exhibit a range of variability that exceeds the probable error in any particular path by an order of magnitude, as illustrated by Fig. 14. The net displacement of the Stream axis between 70 and 71W is smaller than the average north-south displacement in the paths over the region of observation. Thus the node, originally located at 70W, has moved toward the west. This slow motion of the node is also visible in the airtracks (Figs. 5 and 6).

Several qualitatively different regimes of variability in space and time can be isolated, primarily because they are associated with different scales of motion. We represent the paths by the function $y=Y(X,t)$, where X, y and t are longitude, latitude and time, respectively. Then the local heading of the Stream at a given longitude and time is defined as

$$\vartheta(X,t)=\tan^{-1}[(\partial Y/\partial X)_t] \text{ (positive north from east),}$$

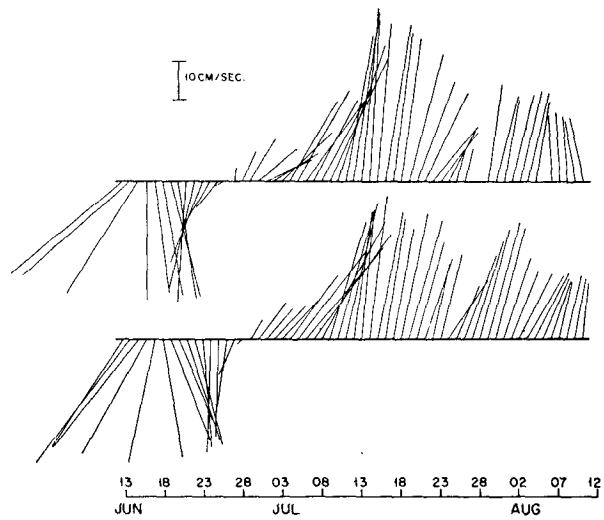

FIG. 10. Low-pass filtered velocity vectors, plotted daily: upper, mooring, 305; lower, 304.

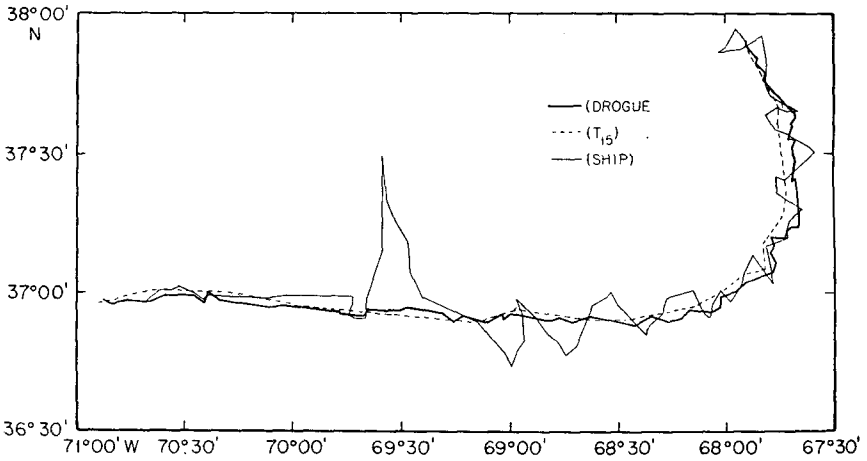

FIG. 11. Comparison between T_{15}, drogue position, and ship's path.

and the local radius of curvature is given by

$$K^{-1}(X,t)=\{(\partial^2 Y/\partial X^2)/[1+(\partial Y/\partial X)^2]^{\frac{3}{2}}\}^{-1}.$$

The local displacement velocity is given by $(\partial Y/\partial t)_x$. The time and space scales of the motion can be measured in terms of these quantities and their derivatives, the rotation rate $(\partial\vartheta/\partial t)_x$, the radius of curvature K^{-1}, and the displacement velocity $(\partial Y/\partial t)_x$. These quantities have been determined graphically from the path and by finite-difference methods from the digitized paths. Except for the case of the curvature, for which the finite-difference estimate is unreliable, the agreement between the two methods is good. If the variability is interpreted as a wave-like motion, the corresponding period and wavelength are found by multiplying the scales by 2π. The above quantities are to be interpreted as the time or distance over which the quantity in question, position or orientation, changes by order one.

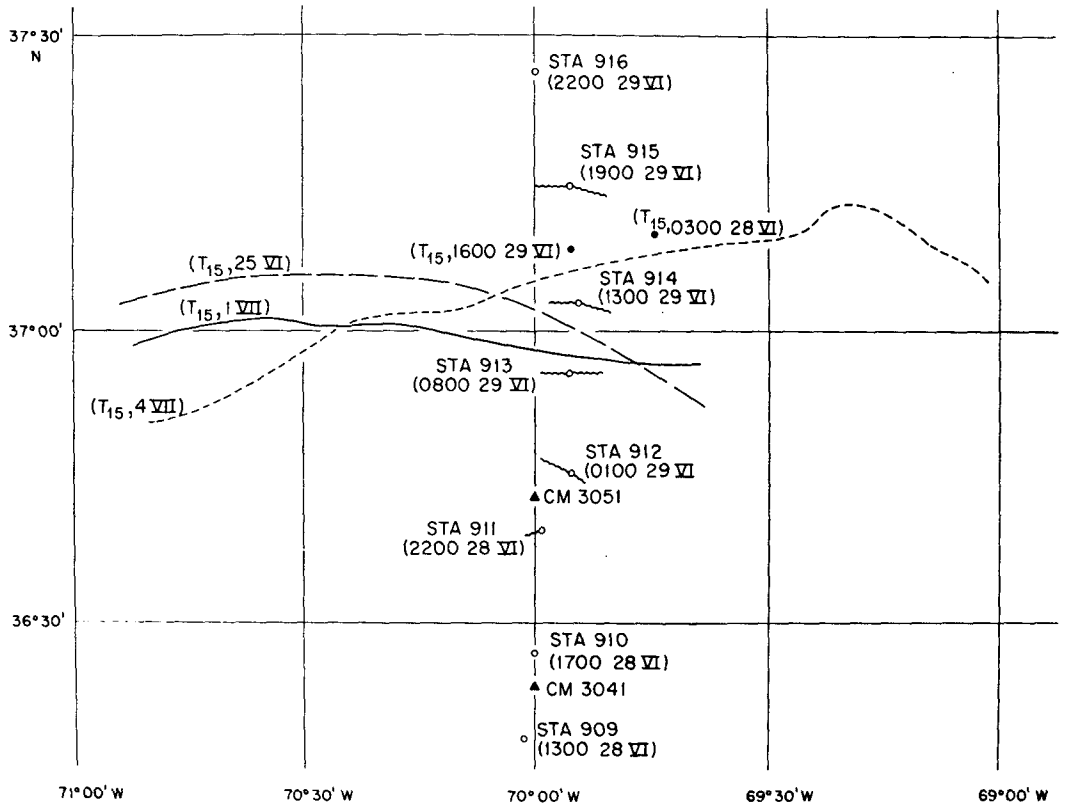

FIG. 12. Data relating to the hydrographic section (Stations 909–916).

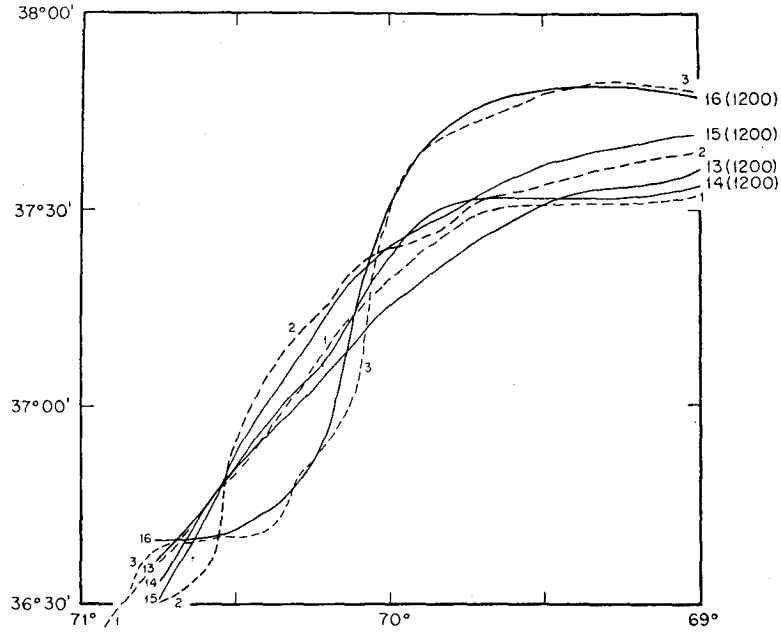

FIG. 13. Comparison between three shiptracks (dashed lines) [1, from 1500 on 13 July to 0200 on 14 July; 2, from 1900 on 14 July to 0600 on 15 July; 3, from 0000 to 1345 on 16 July] and the four corresponding interpolated paths (solid lines) at 1200 on 13, 14, 15, 16 July.

These length, time and velocity scales can, in turn, be used to define or specify a class of motions of the Stream axis.

A comparison of the paths of 4, 7, 12 and 17 July, in Fig. 15, shows the secular change in the overall heading of the Stream was 70°. The cyclonic rotation of the path over the entire region is associated with length scales of 250–350 km, as measured by the radius of curvature of the path. The time scale for this secular change can be estimated from the rate of rotation of the path orientation to be $5\pm2\times10^{-7}$ sec^{-1} (13 ± 3 days). The velocities associated with the local northward displacement of the path in the region of observation range from 0 to 8 cm sec^{-1}, and is consistent with the other scales. In addition to the large-scale secular behavior, the detailed path information can resolve processes of smaller scale both in time and space.

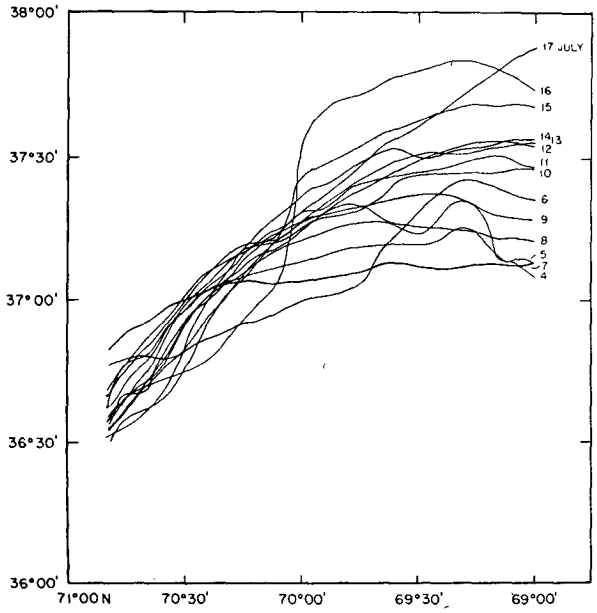

FIG. 14. Composite of interpolated instantaneous paths at 1200 on 4–17 July.

The sequence of paths from 13 to 17 July (Fig. 16) illustrates the rapid development and disappearance of a single local wavelike disturbance of the path. Between 15 July (1200) and 16 July (1200) the path of the Stream was displaced to the north, east of 70W, and to the south, west of 70W. The motion then reversed to leave the path essentially undisturbed 24 hr later. The wavelength of the disturbance is 250 ± 20 km; the corresponding scale is approximately 40 km. The displacement velocities are as great as 22 ± 4 cm sec^{-1}; the time scale is the order of a day (local rotation rate $\sim5\pm4\times10^{-6}$ sec^{-1}).

A small-scale local wavelike disturbance, illustrated in Fig. 17, was observed between 4 July (0000) and 6 July (1200). The displacement between successive paths is on the limit of error but the net displacement is unambiguous. The disturbance is seen to grow and then either decay into longer spatial scales or be advected out of the region. The displacement velocities are small (5 ± 2 cm sec^{-1}) and the spatial scale is between 15 and 30 km, comparable with the width of

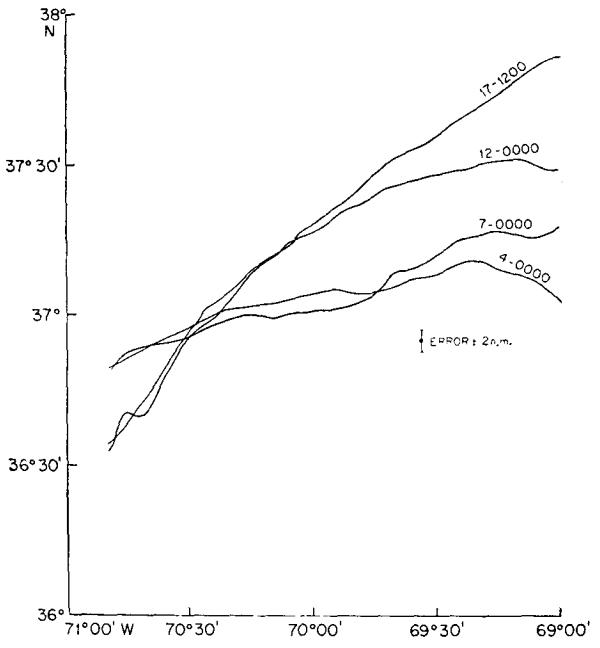

FIG. 15. Secular change in the path orientations at 0000 on 4, 7 and 12 July and at 1200 on 17 July.

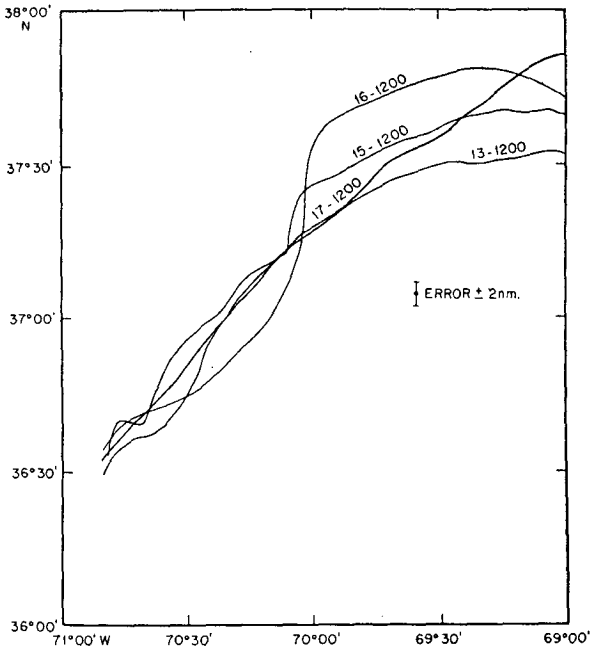

FIG. 16. Development and disappearance of S-shaped feature over the period 13–17 July.

the Stream. It is not clear that these motions will correspond to a meandering of the structure of the Stream; they may be restricted to the near-surface layers.

Since our detailed observations were limited to a region approximately 180 km wide, we are unable to trace these smaller scale disturbances over larger spatial scales. The appearance of energetic small-scale structure which may disappear into larger scale structures is tantalizing but we are unable to document that behavior conclusively.

b. Airtrack and shiptrack intercomparisons

The airborne radiometer measurements determine the horizontal temperature gradients in the first few millimeters of the surface layer of the ocean. The position of these gradients may be affected by a number of environmental factors in addition to the position of the deeper thermal structure of the Gulf Stream, each perhaps with characteristic space and time scales. A comparison between the various shipboard measurements of the surface and near-surface temperature structure reveals some of these scales.

If the features in the airtracks, shown in Fig. 1, are used to define phase lines as with wavelike disturbances, the observed eastward migration of the meander pattern can be identified with a phase velocity of 5–8 cm sec^{-1}. This value is consistent with that obtained by Hansen (1970) from the ESSA paths. It is not possible to construct an envelope of paths from these data as only a single event occurred within the time span of the data. However, it does appear that the large meander grew locally in space and time, rather than increasing linearly with downstream distance as suggested by Hansen (1970).

There is an obvious similarity, illustrated in Fig. 18, between the long ship path, taken between 17 and 20 July, and the flight tracks of 15 and 17 July. The large meander to the east of 70W is indicated by both tracks.

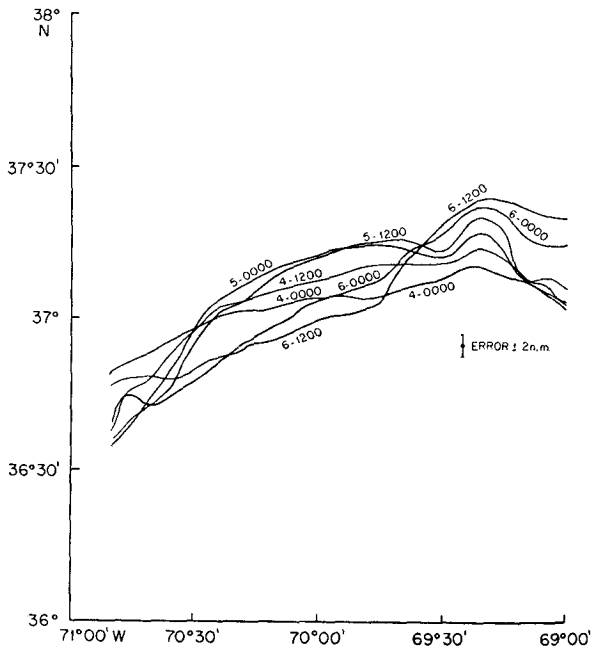

FIG. 17. Small-scale waves over the period from 0000 on 4 July to 1200 on 6 July.

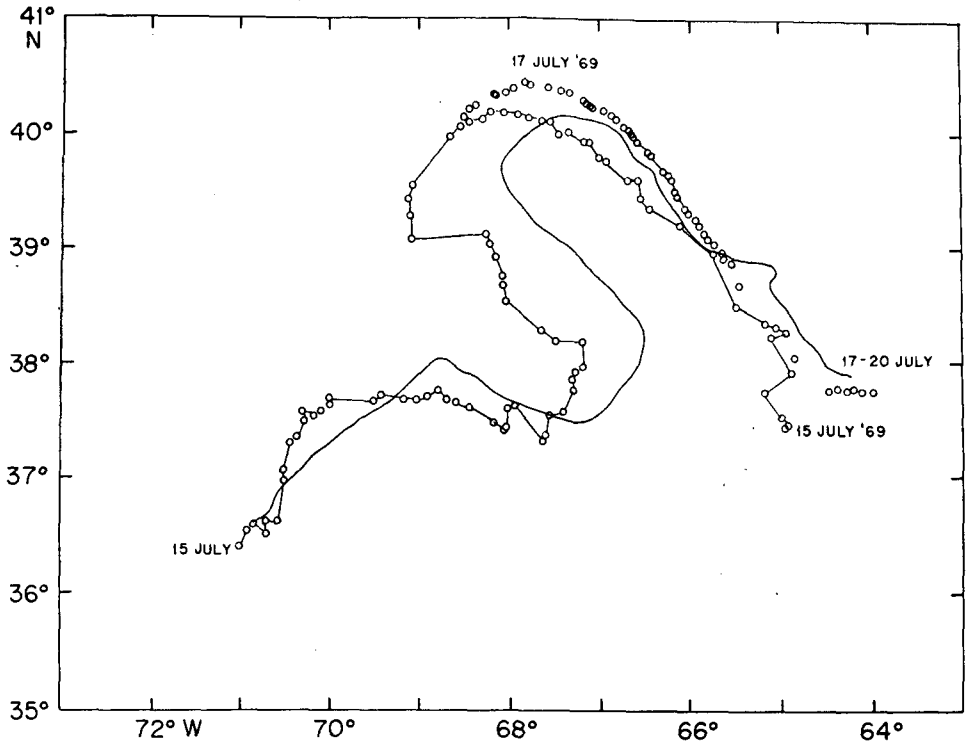

FIG. 18. Comparison between the airtracks (ΔT_a) of 15 and 17 July and the long shiptrack of 17–20 July (T_{15}).

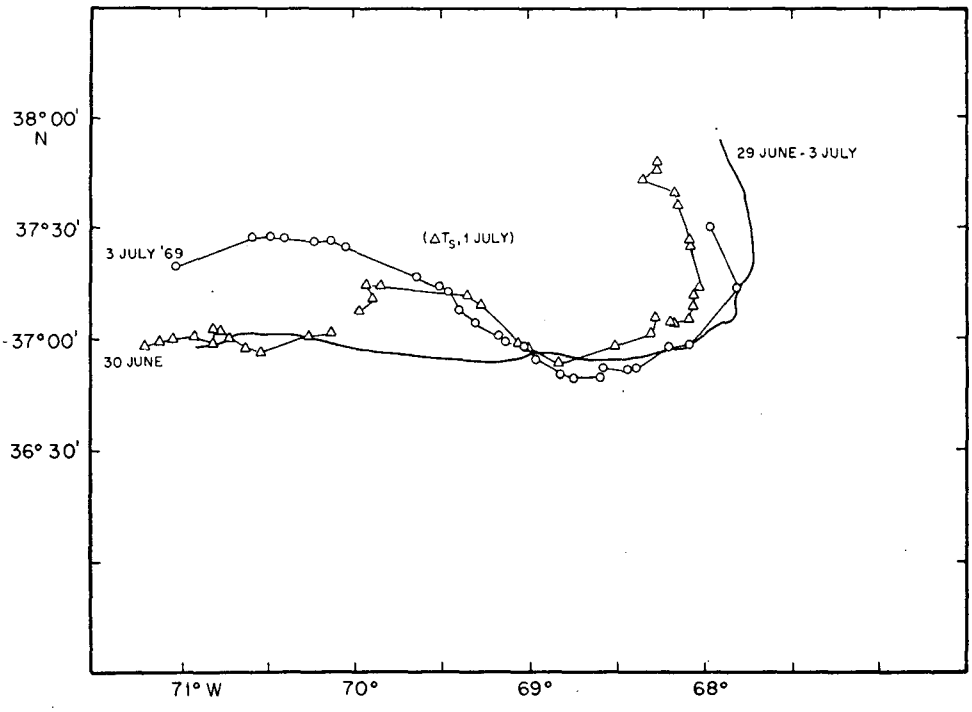

FIG. 19. Comparison between the shiptrack (T_{15}) of 29 June–3 July and the airtracks (ΔT_a) of 30 June and 3 July (ΔT_s of 1 July was determined from ship observations).

A detailed comparison is impossible since the paths are not synoptic; the flight track shown for 15 July required 12 hr, whereas the shiptrack required 3 days. The horizontal displacement of the airtrack from the shiptrack is not uniform along the paths, varying from 50 km to the right (looking downstream) to 200 km to the left. Part of the displacement may be due to the time difference between the paths but certainly not all of it. The maximum speed of displacement of the Stream axis found from the instantaneous paths is 25 cm sec^{-1} which might account for 100 km of the observed displacement.

A similar comparison of the airtracks of 30 June and 3 July and the shiptrack of 1–3 July is shown in Fig. 19. Again the displacement of the airtrack relative to the shiptrack is predominantly shoreward although it is not uniform, ranging from 15 km to the right up to 100 km to the left. During the shiptrack of 2 July, a search was made for the maximum surface temperature gradient. It was found 50 km to the north of the 15C isotherm at 200 m, consistent with the airtrack of 3 July. The position of the gradient ΔT_s is shown in Fig. 17. Intercomparisons of the more detailed thermal structure are given below.

A comparison of the long shiptrack of 25–26 June with the airtrack of 24 June is shown in Fig. 20. The airtrack of 24 June shows a great deal of fine-scale structure which is completely absent from the shiptrack. The spatial scale of these features is between 30–50 km. Since features of this spatial scale were resolved in the dense lines of shiptracks, they should be resolved in the longer shiptracks as well. This suggests that there is little vertical coherence in the thermal structure over 200 m for these smaller spatial scales, in agreement with the discussion of Hansen and Maul (1970).

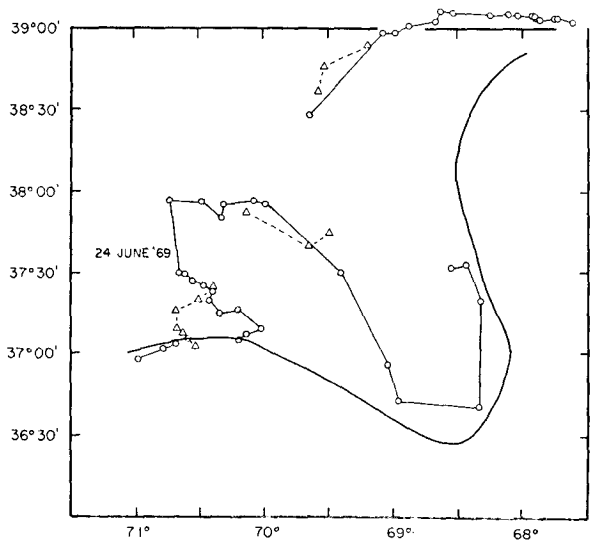

FIG. 20. Comparison between the shiptrack (T_{15}) of 25–27 June and the airtrack (ΔT_s) of 24 June.

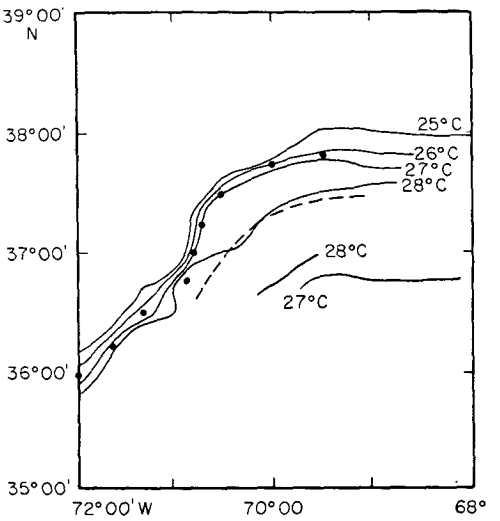

FIG. 21. Comparison between the interpolated T_{15} at 1200 on 11 July (dashed line) and the interpolated surface isotherms (solid lines) from the airtrack of 11 July. [The solid dots approximate ΔT_s values.]

A few comparisons are possible between the time-interpolated instantaneous paths and the airtracks. In Fig. 21 a comparison is shown between the instantaneous path of 11 July and the airtrack of T_s. The agreement between the two, in terms of a separation normal to the path is within 30 km. The isotherms determined along the airtrack are shown as well. A detailed comparison between the thermal structure of the surface layer is not possible since shipboard observations of the surface temperature do not range over a sufficient area in comparison with the airtrack data.

The detailed comparisons between available corresponding data show little coherence over scales of tens of kilometers. This is partly due to the inadequacy of the data; there is no fine-scale sampling over the region either by ship or air to generate a synoptic map of the surface temperature field. Over the larger scales of hundreds of kilometers, there is considerable coherence between the maximum surface temperature gradient and the maximum gradient in the deeper layer, T_{15}. The surface gradient is usually displaced 20–40 km to the shoreward side of the Stream but the displacement is not uniform along the path. The scales of motion associated with the large meanders of the Stream are approximately represented by the airtracks of the surface gradient. These observations are certainly consistent with the statistical analysis done by Hansen and Maul (1970). They found that maximum surface temperature gradient was observed shoreward 14.5 km, from T_{15}, on the average. Hansen and Maul performed a running average of their paths over 20 km along the path. A similar average, where possible, does reduce the mean separation in our data. Hansen and Maul suggest that phenomena of the scale of 30–50 km in the surface temperature gradient are not generally coherent with

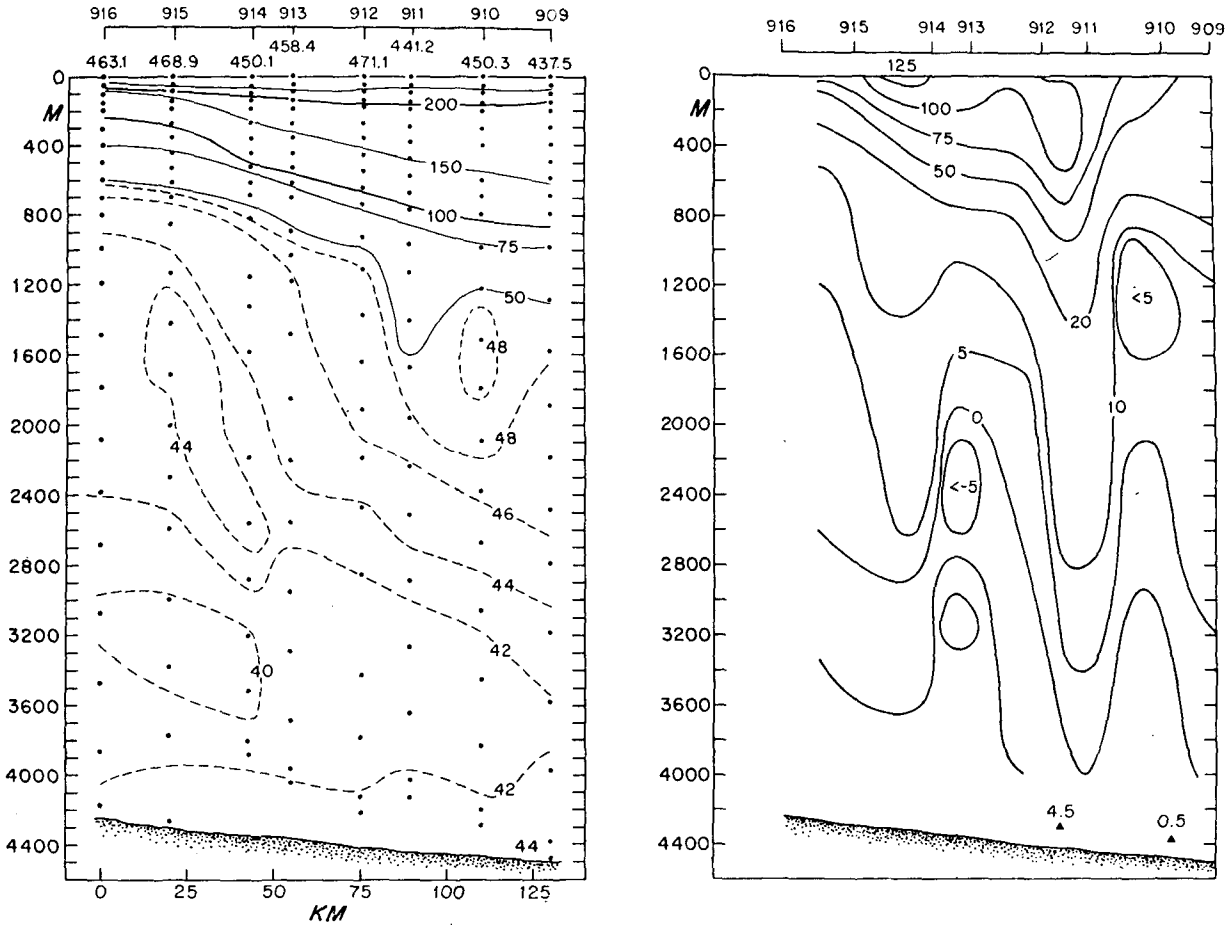

FIG. 22. Specific volume anomaly (left, $10^5\ \delta$) and geostrophic velocity relative to zero bottom velocity (right, cm sec^{-1}); the solid triangles are easterly components of averaged current meter velocity.

the meandering of the deep thermal structure of the Stream. The data presented here certainly bear this out as well.

c. *Geostrophic calculations*

The eight hydrographic stations bracket the four moored current meters and span the core of the Stream. The plot of the specific volume anomaly shown in Fig. 22 is typical of sections across the Stream, as is the computed geostrophic velocity profile relative to zero bottom velocity. The volume transport, relative to zero bottom velocity, is computed to be $77\pm7\times10^6$ m^3 sec^{-1}. Each 1 cm sec^{-1} of horizontally uniform bottom velocity adds 6×10^6 m^3 sec^{-1} to the transport. A comparison of volume transports for the Gulf Stream in the vicinity of 70W, shown in Table 2, indicates that the value of $77\pm7\times10^6$ m^3 sec^{-1} is significantly lower than other estimates of the transport. The motion of the Stream during the hydrographic section is ambiguous (Fig. 17). However, the effects of curvature on the geostrophic equation and the possible motion of the Stream during the measurement period will not account for the discrepancy in transport. Warren and Volkmann (1968) have suggested that the imprecision in the definition of the free seaward (southern) boundary of the Stream tends to an uncertainty of 20–25% in transport. For the section discussed here, no direct estimate of the additional transport to the south of the most southerly station can be made. It is clear, however, that an additional transport of $16\text{–}20\times10^6$ m^3 sec^{-1} would bring the transport values in agreement with previous estimates.

The parameters of interest for the theoretical models of the quasi-geostrophic meandering of the Stream are the moments, or averages across the section, of the velocity distribution, its square, and the bottom velocity. These moments, denoted by $\langle v\rangle$, $\langle v^2\rangle$ and $\bar{v}$, respectively, are shown in Table 2. The hydrographic data only give information about the vertical shear of the geostrophic velocity, and thus only $\langle v-v_B\rangle$ and $\langle(v-v_B)^2\rangle$, where v_B is the velocity at the bottom, are determined. The absolute velocity can only be determined by some complementary measurements. An estimate of the bottom velocity, and the corresponding

TABLE 2. Gulf Stream volume transports.

Observer†	Transport to bottom ($\times 10^6$ m^3 sec^{-1})	$\langle v-v_B \rangle$ (cm sec^{-1})	$\langle (v-v_B)^2 \rangle^{\frac{1}{2}}$ (cm sec^{-1})	$\langle v \rangle$ (cm sec^{-1})	$\langle v^2 \rangle^{\frac{1}{2}}$ (cm sec^{-1})	v (cm sec^{-1})	Method
Warren and Volkmann (1968)	101	13.5	—	15	30	1.5	Hydrographic
69°00′W,	—	—	—	—	—	—	swallow floats
37°30′N	—	—	—	—	—	—	
Barrett and Schmitz	90	18	38	—	—	—	Hydrographic
	87	17	34	—	—	—	Hydrographic
67°30′W,	119	23	41	—	—	—	Hydrographic
37°30′N	165	11	—	27	44	16	Transport float
(6 sections)	203	31	—	27	49	−4	Transport float
	129	24	—	19	41	−5	Transport float
Fuglister (1963)	137	16	34	—	—	—	Hydrographic
68°30′W,	—	—	—	—	—	—	
37°30′N	—	—	—	—	—	—	
*Chain**	77	15	21	—	—	—	Hydrographic
70°00′W,	227	15	—	45	57	30	Hydrographic and
37°30′N	—	—	—	—	—	—	moored current meter data

† Position given is the approximate location of the Stream axis.
* Reported in this paper.

moments of the absolute velocity distribution determined from the moored current meter data, included in Table 2, is discussed in the following section.

It should be noted that there is significantly less variability in the computed average velocities and their square (mean momentum flux) relative to the bottom than in the quantities derived from the absolute velocity. Apparently the mean baroclinic flow, determined solely by the net cross-stream density differences, is less variable than the total flow, including the barotropic component.

d. Current meter intercomparisons

The moored current meter data can be compared in various ways with the near-surface observations of the position of the Stream. Schmitz *et al.* (1970) have compared the integrated north-south velocity, the virtual displacement, from the current meters with the latitudinal movement of the airtrack position (ΔT_s) at 70W. There is a clear visual coherence between the displacement of ΔT_s and the virtual displacement at the current meters although the latter are nearly an order of magnitude larger in scale. A more detailed comparison between the current meter data and the displacement of the instantaneous paths based on the quasi-geostrophic time-dependent model is discussed by Luyten and Robinson (1974).

In principle, the moored current meter data can be used to determine the absolute velocity in conjunction with the hydrographic section. The motion having frequencies greater than the local inertial frequency cannot be quasi-geostrophic so that the low-pass filtered records (Section 3d, Fig. 9) give the appropriate currents for comparison. The problem is as always in such comparisons to decide the time scale appropriate to the hydrographic data. A time average over the duration of the hydrographic section gives mean east and north components

$$\left.\begin{array}{ll} 3041 & (+0.5, -1) \text{ cm sec}^{-1} \\ 3051 & (4.5, 7) \text{ cm sec}^{-1} \end{array}\right\}$$

at 200 m from the bottom. The mean easterly flow over this period, as shown at the current meter positions in Fig. 22, is consistent with the geostrophic shear calculation in the sense that the largest velocity corresponds to the most energetic part of the geostrophically calculated flow. From two points it is difficult to reconstruct the bottom velocity profile to estimate the contribution to the transport. This contribution could be on the order of $3\text{–}27 \times 10^6$ m^3 sec^{-1}, based on the range of observed bottom velocity. The geostrophic section was made during a period when the observed currents were small. Even during this quiescent period there was considerable cross-stream flow whose explanation requires a more specific model of the motion of the Stream, as discussed by Luyten and Robinson (1974). However, some of the results will be included here for completeness.

The Stream is imagined to move in a vertically coherent and inextensible fashion as it meanders so that the velocity observed at the current meter should be compounded of the bottom velocity of the Stream profile together with the components of velocity due to the motion of the axis. The bottom velocity of the Stream computed in this manner for the period of time when the instantaneous paths are available (4–17 July) is 30 cm sec^{-1}. This value is 50% larger than any previously reported estimate of the bottom velocity.

The period over which the bottom velocity was determined corresponds to an energetic part of the current meter records (Fig. 9) and is associated with variability or periods long ($\sim$30 days) with respect to the averaging interval. Without observations of the path of the Stream over these longer periods, it is not possible to determine the bottom velocity of the Stream from the current meter velocities. However, in the absence of such observations, we have included this estimate, with the above reservations, in Table 2. The corresponding moments of the absolute velocity profile are computed as

$$\langle v\rangle = \langle v - v_B\rangle + \bar{v},$$
$$\langle v^2\rangle \approx \langle (v-v_B)^2\rangle + 2\bar{v}\langle v - v_B\rangle + \bar{v}^2,$$

where $\langle v_B\rangle = \bar{v}$ is the cross-stream average bottom velocity.

5. Conclusions

We have investigated the space and time variability of the Gulf Stream in the vicinity of the 70th meridian by a variety of oceanographic techniques. The picture of the Stream that emerges is one of change over the full range of space and time scales within the limits of the observations. The focus of the analysis of these data is necessarily deterministic since the scope of the observations is too limited for reliable statistical inference. The various techniques give a consistent measure of the variability where the appropriate scales overlap.

The large-scale variability is consistent with the classic work of Iselin (1938) and Fuglister (1963)—the Gulf Stream is a narrow intense current which meanders as a coherent structure in the sense that the strong velocity core near the surface moves together with the near surface thermal structure. The close correspondence between the path of the 200 m drogue and the simultaneous T_{15} track is further evidence that the meandering is vertically coherent over small scales as well. We examine this question of vertical coherence in greater detail in Part II, applying a specific kinematic model of the velocity field to the path and deep current meter observations. Whether this coherence obtains throughout the water column can only be answered by a time series of vertical profiles of the current.

There is, however, considerably more variability in the observed path of the Stream (T_{15}) on smaller time and space scales than was suspected by Iselin (1938), Fuglister and Worthington (1951) or Fuglister (1963). While our detailed observations of T_{15} do not extend over a sufficiently long period of time to document the complete development of a large-scale meander, the two-week time series of paths near 70W indicates that large-scale changes in the position of the Stream can occur over periods of a day with displacement velocities several times larger than were inferred by Fuglister (1963) and Hansen (1970). Three regimes of path variability can be identified, each with characteristic space and time scales: 1) slow, long-spatial-scale, secular changes; 2) the intermediate-scale variation due to the more or less rapid passage of a feature; 3) small-scale wavelike disturbances. The scales associated with these motions are summarized in Table 1. However, without observations of this nature over longer periods of time the statistical importance of these phenomena cannot be determined.

The aerial surveys of the surface expression of the Stream are in agreement, over large scales, with the deep thermal structure (T_{15}) although the position of ΔT_s is typically observed 30 km shoreward from T_{15}. It is evident that a sampling interval of two days is sufficient to resolve the evolution of meanders over large scales.

The moored current meter records from 200 m above the sea bottom exhibit large velocities (44 cm sec^{-1}) and a great deal of variability over time scales long with respect to a day. The deep velocities under the Stream are not colinear with the strong baroclinic flow of the Stream, so that the current meter velocities do not directly determine the barotropic flow. There is no simple prescription for averaging these data to determine the bottom velocity of the Stream. The quasi-geostrophic model of Robinson *et al.* (1973) relates the variability of the deep flow to the motion of the Stream axis to give an estimate of the bottom velocity of the Stream (Luyten and Robinson, 1974). The hydrographic section across the Stream is typical of sections in this vicinity and does not reflect strong flow near the bottom. Furthermore, other records from near-bottom-moored current meters in the vicinity of the Stream exhibit variability of this same scale and magnitude, suggesting that these larger velocities are not atypical (Luyten and Schmitz, 1973). Again we must say, however, that observations over much longer periods of time are required to determine the statistical nature of these events.

The Gulf Stream exhibits space and time variability over many scales. Our purpose here has been to examine the relations between the time and space scales of variability, without drawing conclusions about the dynamical role of the variability in determining the evolution of the Stream. Some conclusions of this nature relating to the study are discussed in Part II (Luyten and Robinson, 1974).

Acknowledgments. The work reported here was carried out with the support of the Office of Naval Research under contracts with Harvard University (ARR and JRL, N00014-67-A-0290-00113717) and with the Woods Hole Oceanographic Institution (FCF and JRL, N00014-66-C0241, NR083004). Their support is gratefully acknowledged. We would like to thank Captain Davis and his crew on the R/V *Chain* for their assistance.

REFERENCES

Crease, J., 1962: Velocity measurements in the deep water of the western North Atlantic. *J. Geophys. Res.*, **67**, 3173–76.

Fomin, L. M., 1964: *The Dynamic Method in Oceanography*. New York, Elsevier.

Fuglister, F. C., 1963: Gulf stream '60. *Progress in Oceanography*, Vol. 1. New York, Pergamon Press, 265–383.

——, and A. D. Voorhis, 1965: A new method of tracking the Gulf Stream. *Limnol. Oceanogr.*, Suppl. **10**, 115–124.

——, and L. V. Worthington, 1951: Some results of a multiple ship survey of the Gulf Stream. *Tellus*, **3**, 1–14.

Hansen, D. V., 1970: Gulf Stream meanders between Cape Hatteras and the Grand Banks. *Deep Sea Res.*, **17**, 495–511.

——, and G. A. Maul, 1970: A note on the use of sea surface temperature for observing ocean currents. *Remote Sensing Environ.*, **1**, 161–164.

Iselin, C. O'D., 1938: Report on the variations in the transport of the Gulf Stream system. *Pap. Phys. Oceanogr. Meteor.*, **8**, 3–40.

Luyten, J. R., and A. R. Robinson, 1974: Transient Gulf Stream meandering. II: Analysis via the quasi-geostrophic model. *J. Phys. Oceanogr.*, **4**, 256–269.

——, and W. J. Schmitz, 1973: Scales of variability in the deep flow near the Gulf Stream. (In preparation.)

Parker, C. E., 1972. Some direct observations of currents in the Gulf Stream. *Deep Sea Res.* **19**, 879–893.

Robinson, A. R., 1971: The Gulf Stream. *Phil. Trans. Roy. Soc. London*, **A270**, 351–370.

——, J. R. Luyten, and F. Flierl, 1973: On the theory of free jets: A quasi-geostrophic time dependent model. (To appear.)

Schmitz, W. J., A. R. Robinson and F. C. Fuglister, 1970: Bottom velocity observations directly under the Gulf Stream. *Science*, **160**, 1192–1194.

Swallow, J. C., 1971: The *Aries* current measurements in the western North Atlantic. *Phil. Trans. Roy. Soc. London*, **A270**, 451–460.

Warren, B. A., and G. H. Volkmann, 1968: Measurement of volume transport of the Gulf Stream south of New England. *J. Marine Res.*, **26**, 110–119.

Wilkerson, J. C., and V. E. Noble, 1970: Time-space variations of the Gulf Stream boundary as observed by airborne remote sensing techniques. *Proc. 6th Symp. Remote Sensing of the Environment*, Vol. 2, University of Michigan, Ann Arbor, 671–708.

Worthington, L. V., 1954: Three detailed cross-sections of the Gulf Stream. *Tellus*, **6**, 116–123.